ANNALS OF GEOPHYSICS, 67, 3, OC322, 2024; doi:10.4401/ag-9102
OPEN ACCESS

Silica spherules in Late Pleistocene-Holocene glaciomarine sediments from the Ross Sea, Antarctica: insights into the formation and significance

Alessio Di Roberto[*,1], Paola Del Carlo[1], Antonella Bertagnini[1], Ester Colizza[2], Massimo Pompilio[1], Federico Giglio[3], Fabio Florindo[4]

(1) Istituto Nazionale di Geofisica e Vulcanologia, Sezione di Pisa, Via C. Battisti 53, 56125 Pisa, Italy
(2) Dipartimento di Matematica, Informatica e Geoscienze, Università di Trieste, Via E. Weiss 2, 34127 Trieste, Italy
(3) Istituto di Scienze Polari – Consiglio Nazionale delle Ricerche, Via P. Gobetti 101, 40129 Bologna, Italy
(4) Istituto Nazionale di Geofisica e Vulcanologia, Via di Vigna Murata 605, 00143 Roma, Italy

Article history: received April 22, 2024; accepted July 6, 2024

Abstract

In this study, we investigate silica spherules with a diameter <1.25 mm from sediment cores retrieved from the northern Drygalski Trough, during the Italian Antarctic Research Programme (PNRA) expeditions in 1999 and 2002. In the past, these unique spherules have been a subject of interest due to their distinctive characteristics. Despite previous hypotheses on their origin, a comprehensive discussion on their formation mechanism and implications in marine sediments was lacking. Our analysis encompasses the depositional environment, morphology, internal texture, major element composition, and age determination through radiocarbon dating (^{14}C) and ^{40}Ar-^{39}Ar dating of spherule-containing sediments. By integrating our findings with a critical review of existing literature, we propose that spherules form by cyclical chemical precipitation of silica when silica-rich freshwater mixed with seawater during extensive events of ice melting. We also tentatively suggest that these spherules possibly represent a proxy for significant meltwater production and discharge into the Antarctic Ocean.
This research contributes to a better understanding of silica spherules in polar marine environments and their implications for past climate conditions.

1. Introduction

Micron- to millimetre-sized silica-rich spherules form through various natural processes and have been found in diverse geological records. These processes include lightning strikes within volcanic eruptive columns [Genereau et al., 2015], the cooling and rapid alteration of volcanic glass droplets in eruptive plumes [Lefèvre et al., 1986; Spadaro et al., 2002; Porritt et al., 2012], cloud-to-ground lightning strikes [Pasek et al., 2012], as well as meteorites impacts on silica-rich terrain [Genge et al., 2008; Glass and Simonson, 2013]. However, there exists a distinct group of silica spherules that cannot be attributed to these "conventional" processes based on their

chemical composition, morphology, and internal texture. These unique spherules have been repeatedly identified in glaciomarine sediments from the Ross and Weddell Seas in Antarctica, with hypotheses proposed for their formation mechanism [Perry, 1999; Gerard-Little et al., 2006; Yeh et al., 2012], in some cases only tentatively [Weiterman and Russell, 1986]. Despite these proposals, a comprehensive discussion on the formation mechanism and the significance of their presence in marine sediments is still lacking.

In this study, we present findings on silica spherules with a diameter <1.25 mm discovered in Late Pleistocene-Holocene marine sediments from the Ross Sea during the 1999 and 2002 oceanographic expeditions of the Italian Antarctic Research Programme (PNRA). Our analysis includes the depositional environment of the spherules, their morphology, internal texture, major element composition, and age determination through radiocarbon dating (^{14}C) and ^{40}Ar-^{39}Ar dating of the spherule-containing sediments. By integrating our data with a comprehensive review of previous studies on silica spherule occurrences, we put forth a hypothesis regarding the formation mechanism of these spherules and suggest their potential utility as a proxy for significant meltwater production and discharge into the Antarctic Ocean.

2. Study area

The sediment cores investigated were obtained north of Coulman Island in the northern Drygalski Trough, which follows a paleo-ice stream that is oriented SSW/NNE and runs along the axis of the trough (Fig. 1). This particular section of the trough reaches depths of approximately 600 m. The morphology of the region is notably complex, characterised by drumlins, mega-scale glacial lineations, and iceberg furrows running parallel to the trough axis [Shipp et al., 1999]. During the Last Glacial Maximum (LGM), the grounding line was situated on the mid-outer shelf just north of Coulman Island. However, by approximately 13,000 ka BP, the grounding line had retreated from this maximum position [Livingstone et al., 2012; Anderson et al., 2014 and references therein]. The Drygalski

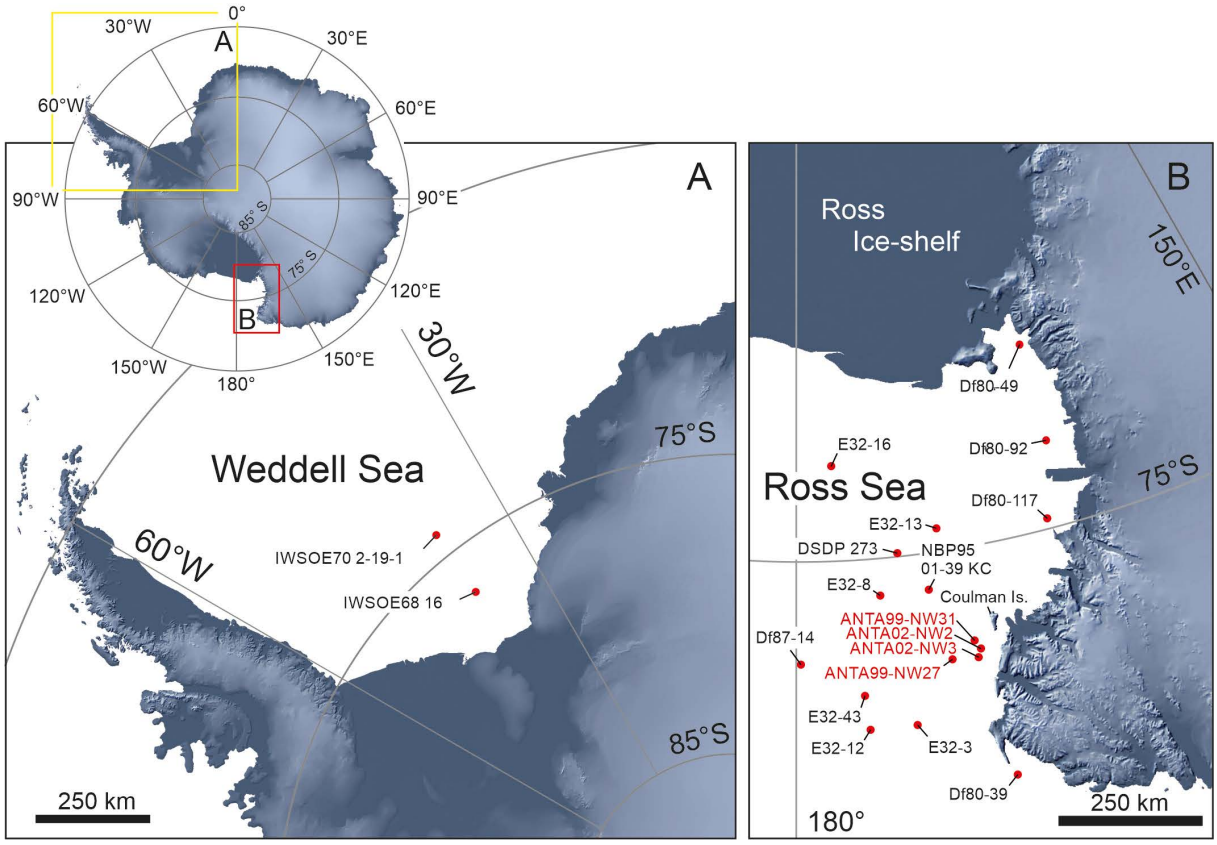

Figure 1. Maps of A) Weddell Sea, and B) Ross Sea, showing the location of cores in which silica spherules were found. The cores studied in this work are highlighted in red. The figure is based on a NASA map by R. Simmon [data from the Radarsat Antarctic Mapping Project, T. Scambos, C. Shuman, and M.J. Siegert].

Trough plays a vital role as a conduit for warm water masses to flow onto the continental shelf and facilitates the transportation of dense shelf water, specifically High Salinity Shelf Water (HSSW), towards the shelf break from source regions further south [Budillon et al., 2011].

3. Methods of investigation

We examined cores retrieved by gravity corer in the Ross Sea during the 1999 and 2002 oceanographic expeditions of the PNRA (Fig. 1). Samples of 20 cm^3 were collected at 5 cm intervals along the studied cores and sieved at one φ interval (where $\varphi = -\log_2 D$ with D = the particle diameter) ranging from −3 φ (8 mm) to +5 φ (0.032 mm). All grain-size fractions were inspected under the stereomicroscope, and the spherules were hand-picked. The presence of spherules was examined down to +5 φ using a scanning electron microscope (SEM). For each sample, the number of spherules per gram of dry weight was determined, as presented in Table 1.

Core	Depth [cm b.s.f.]	Grain-size	Sperule n°	Grams	Sperule/g
ANTA02-NW02	133	1000-125 µm	2	31.33	0.06
ANTA02-NW03	1	1000-125 µm	10	19.94	0.50
ANTA02-NW03	12	1000-125 µm	7	23.70	0.30
ANTA02-NW03	103	1000-125 µm	1	13.86	0.07
ANTA99-NW27	18.5	500-250 µm	4	10.55	0.38
ANTA99-NW27	25.5	500-250 µm	1	1.92	0.52
ANTA99-NW27	45.5	500-250 µm	1	9.86	0.10
ANTA99-NW27	55.5	500-125 µm	7	10.16	0.69
ANTA99-NW27	168.5	500-250 µm	1	6.35	0.16
ANTA99-NW31	14.5	500-250 µm	4	2.95	1.36
ANTA99-NW31	41.5	500-250 µm	6	4.60	1.31
ANTA99-NW31	63.5	1000-250 µm	1	6.80	0.15
ANTA99-NW31	70	1000-125 µm	50	25.75	1.94
ANTA99-NW31	71.5	1000-500 µm	11	11.10	0.99
ANTA99-NW31	80	1000-125 µm	39	28.68	1.36
ANTA99-NW31	82.5	1000-125 µm	12	9.58	1.25
ANTA99-NW31	88	1000-125 µm	44	20.82	2.11

Table 1. Number of silica spherules per gram of dry sediment in the studied sequences.

The spherules were photographed, and their shape and internal texture were described using the optical microscope. Subsequently, they were embedded in epoxy resin and prepared as thin sections for internal microtextural observation under a scanning electron microscope (SEM) at the Istituto Nazionale di Geofisica e Vulcanologia (Sezione di Pisa) with a Zeiss EVO MA 10.

The major element composition of the spherules was analysed at the HPHT Laboratory of Istituto Nazionale di Geofisica e Vulcanologia (Sezione di Roma) using a JEOL JXA 8200 electron microprobe equipped with 5 wavelength-dispersive spectrometers (WDS) and an energy-dispersive analytical system (EDS). The instrumental working conditions were as follows: 15 kV accelerating voltage, 12 nA beam current, 5 µm electron beam diameter, with 10 s and 5 s acquisition time for peak and background, respectively. For each sediment sample, 5 spherules were randomly selected, and a minimum of 10 points were analysed from the rim to the core of each spherule. Analytical errors were estimated from mineral and natural glass standards and are typically less than 1% for major elements >10 wt%, less than 5% for major elements 1-10 wt%, and less than 10% for minor elements 0.1-1 wt%.

The determination of biogenic silica on spherules was carried out on samples where the spherules were more abundant, specifically in ANTA99-NW31-71.5 and ANTA99-NW31-88. Each sample underwent analysis twice. Biogenic silica contents were determined following a progressive dissolution method [DeMaster, 1981], followed by colorimetric analysis. A 0.5 M NaOH solution was used as an extractant due to the high concentration of biogenic silica in our samples. The extraction process involved subjecting 20 mg of spherules to extraction at 85°C, with 0.2 ml aliquots taken for analysis every hour for 4 hours. The associated error typically falls within the range of 5-8%.

Age constraints for the sediment layers containing spherules were obtained from previous studies, which included ^{14}C dating of decalcified sediment samples [Colizza et al., 2003] and $^{40}Ar/^{39}Ar$ dating of single k-feldspar crystals from tephra layers [Del Carlo et al., 2015]. Additionally, the sediment layers containing spherules were dated using the AMS ^{14}C dating method on planktonic foraminifera concentrate. Three AMS ^{14}C analyses were performed on mixed benthic foraminifera. The radiocarbon ages were calibrated using the OxCal program, with a reservoir correction ΔR (reservoir age) of 1300 ± 300 years utilized for calibration, as recommended by Berkman and Forman [1996] for Southern Ocean carbonate samples. The calibrated ages are reported in years BP and correspond to a 2σ confidence level.

4. Results

4.1 Abundance, textural characteristics and composition of spherules

Spherules were discovered in four of the nine analyzed sediment cores, specifically in the ANTA99-NW27, ANTA99-NW31, ANTA02-NW02 and ANTA02-NW03 cores. These cores are located approximately between 40 and 80 km north of Coulman Island, in the northern part of Drygalski Trough (Fig. 1). In these cores, the spherules concentration ranges from 0.06 to 2.11 per gram of dry sediment (Table 1). The diameters of the spherules vary from approximately 0.125 mm to 1.25 mm. Most spherules are transparent and colourless, with some exhibiting a pearly lustre. They vary in shape from spherical to ellipsoidal or slightly dumbbell-shaped, with a few resembling apples (Fig. 2a-c). The inner parts of the spherules show a structured appearance with thin, well-defined, concentric layering parallel to the external surface (Fig. 2c-i). No detrital grains, bioclasts, or other particles were observed in the spherules nuclei (Fig. 2c-i). The layers vary in thickness from a few microns to tens of microns, typically thinning with distance from the nuclei (Fig. 2). The external texture is influenced by the inner structure, often displaying exfoliation surfaces. The external surface is smooth at a micron-scale level, occasionally showing wrinkled and micro-pitted surfaces.

The spherules' major element chemical composition is consistent, as shown in(major elements in wt.%). They typically contain around 78-85 wt.% SiO_2 and ≤1 wt.% $Na_2O + K_2O$. The total of the remaining elements (TiO_2, Al_2O_3, FeO, MgO, MnO, CaO, and P_2O_5) never exceeds 1 wt%. The estimated water content, based on the analytical deficit in EMP-WDS analyses, ranges from 15.6 to 21.1 wt%.

The spherules are primarily composed of silica. Biogenic silica analyses indicate that inorganic silica predominates, with biogenic silica accounting for less than 0.5 wt%.

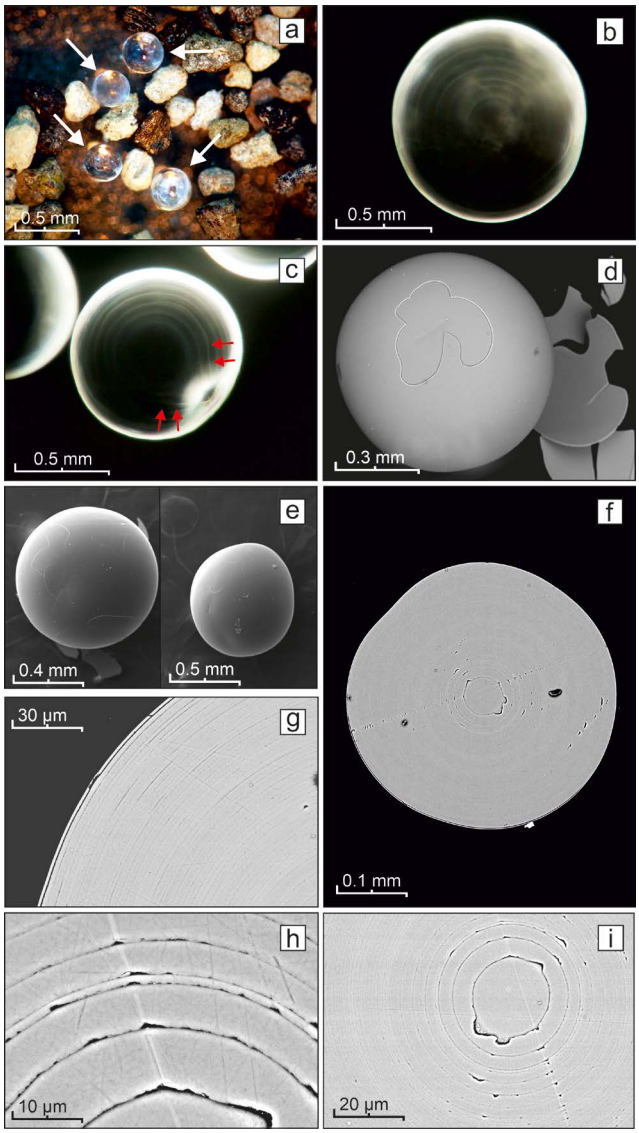

Figure 2. Optical microscope and SEM backscatter images of the spherules identified in the ANTA99-NW27, ANTA99-NW31, ANTA02-NW02 and ANTA02-NW03 sediment cores from the Ross Sea (Antarctica). A) Silica spherules within volcanoclastic sediments of core ANTA99-NW31. B-c) Internal structure of the spherules observed under optical microscope in transmitted light. D-e) Detail of the external and f-i) internal structure of the spherules observed under scanning electron microscope.

	Depth [cm]	SiO_2	St. dev [2σ]	Al_2O_3	St. dev [2σ]	FeO	St. dev [2σ]	MgO	St. dev [2σ]	CaO	St. dev [2σ]	Na_2O	St. dev [2σ]	K_2O	St. dev [2σ]	Total	St. dev [2σ]
NW2	0-1	83.49	1.44	0.04	0.03	0.02	0.03	0.01	0.02	0.03	0.02	0.67	0.07	0.14	0.03	84.38	1.43
	11-12	83.70	0.76	0.04	0.02	0.02	0.03	0.02	0.03	0.01	0.01	0.63	0.05	0.12	0.02	84.54	0.76
	51-52	83.02	0.90	0.02	0.01	0.01	0.02	0.01	0.02	0.01	0.02	0.70	0.04	0.15	0.03	83.92	0.93
	69-70	82.60	0.84	0.04	0.03	0.02	0.02	0.00	0.01	0.02	0.02	0.69	0.04	0.14	0.02	83.51	0.84
NW31	78-79	82.62	1.81	0.04	0.02	0.02	0.03	0.01	0.02	0.00	0.01	0.73	0.08	0.14	0.02	83.56	1.84
	88-89	78.06	5.77	0.13	0.29	0.01	0.02	0.01	0.01	0.02	0.02	0.56	0.20	0.12	0.05	78.91	5.76

Table 2. Average major element composition and standard deviation of silica spherules from ANTA99-NW31 and ANTA02 NW2 cores from Antarctica determined by SEM-EDS and EMPA.

4.2 Depositional environment and age of spherules in the investigated sequences

The four sediment cores in which spherules were discovered primarily consist of glaciomarine sediments ranging from mud to sand. Moreover, these cores contain abundant primary pyroclastic fall deposits and slightly reworked volcaniclastic sands enriched with bioclasts are abundant in these cores. In cores ANTA99-NW27 and ANTA99-NW31, a diamictite layer rich in volcanic fragments is present at the base of the sequences (Fig. 3). Additionally, a minor quantity of iceberg-rafted debris, in the form of oversized clasts known as dropstones, is also observed. The characteristics of the tephra layers suggest that they are fallout primary beds deposited through the water column during Plinian to sub-Plinian eruptions [Del Carlo et al., 2015]. The volcanic eruptions responsible for these deposits have been dated between 137.1 ± 3.4 and ≤12 ka years ago [Del Carlo et al., 2015].

The presence of spherules appears to be independent of sedimentary facies, as they have been identified in all types of sediments except diamictite.

Core ANTA99-NW27 (327 cm) was retrieved at a water depth of 524 m. The lower section of the core (213-327 cm) comprises unstructured diamicton with a limited biogenic fraction. The overlying sediment is homogeneous silty sand with occasional clasts. Towards the upper portion, silty sand with an abundant biogenic fraction (mainly forams and sponge spicules) dominates. Ice-rafted debris is sporadically present throughout. Notably, two layers of volcanoclastic sand to silty sand with inverse to normal grading are observed in this core (refer to Fig. 3). Spherules are found at 168.5 cm and 18.5-55.5 cm within this core. Radiocarbon dating at depths of 231-232 cm and 71-72 cm provides an age between 30.3 and 25.4 ka cal. BP for the lowermost spherule-bearing layer and an age younger than 25.4 ka cal. BP for the uppermost one.

Core ANTA99-NW31 (372 cm) was collected at a water depth of 535 m. The lower section of the core (224-372 cm) is characterised by a mixture of sand, silt, and clay with abundant clasts (diamicton) and a limited biogenic fraction. Moving upwards, the sediment transitions from silty clay to sandy silt and silty sand, with occasional gravel fractions. The biogenic fraction is mainly concentrated in carbonate-rich levels. Two tephra layers are observed at depths of 173-205 cm and 42-61 cm (Fig. 3). Spherules are consistently present between depths of 14.5

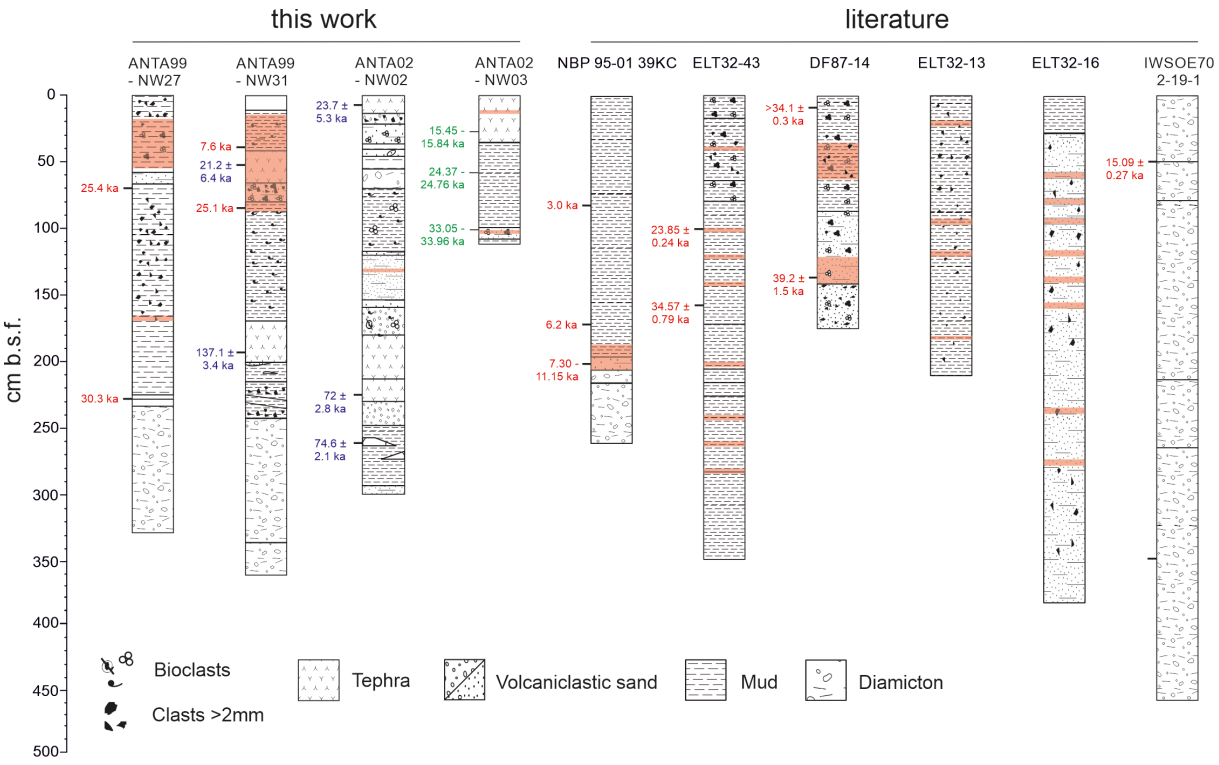

Figure 3. Stratigraphic logs of cores. The sediment intervals in which spherules have been identified are highlighted in red. ^{40}Ar-^{39}Ar [in blue, Del Carlo et al., 2015] and ^{14}C ages [Colizza et al., 2003] of the studied deposits are also shown. ^{14}C ages from this study are in green, and the ^{14}C ages from the literature are in red.

and 89 cm, with a radiocarbon-corrected age estimated to be approximately between 7.6 ka and 24.1 ka cal. BP [Colizza et al., 2003]. A†radiometric age of 21 ± 6.4 ka cal. BP obtained using ^{40}Ar-^{39}Ar dating of the tephra at 42-61 cm [Del Carlo et al., 2015] is consistent with the radiocarbon age.

Core ANTA02-NW02 (302 cm) was collected from a water depth of 588 m and exhibits alternating layers of silty/muddy-volcaniclastic sand, silty clay to sandy silt, and thick tephra layers. Spherules are discovered at a depth of 133 cm within a silty/muddy-volcaniclastic sand layer (refer to Fig. 3). Three corrected radiometric ages were obtained through ^{40}Ar-^{39}Ar dating on k-feldspar crystals within tephra layers sampled at depths of 3.5-4.5 cm, 225-226 cm, and 256-257 cm, yielding ages of 23.7 ± 5.3 ka, 72 ± 2.8 ka, and 74.6 ± 2.1 ka, respectively [Del Carlo et al., 2015; see Fig. 3]. Consequently, a generalised age between 23.7 ± 5.3 ka and 72 ± 2.8 ka is inferred for the sediment containing the spherules.

Core ANTA02-NW03 (113 cm) was retrieved from a water depth of 534 m and is characterized by very dark grey terrigenous and volcanoclastic sand to muddy sand with sparse mm to cm clasts (as shown in Fig. 3). Bioclasts, mainly consisting of foraminifers and bryozoans, are concentrated in certain levels. Spherules are located at a depth of 104 cm within volcanoclastic sand and at depths of 0-12 cm in the reworked upper portion of a tephra layer occurring at depths of 25-35 cm (refer to Fig. 3). Calibrated radiocarbon ages of 33.05-33.96 ka and younger than 15.45-15.84 ka BP were obtained on planktonic foraminifera for the two layers bearing spherules (see Fig. 3).

4.3 Occurrence of silica spherules in other sediment cores from Ross and Weddell Seas

Silica spherules similar to those described in this study have been previously documented in glaciomarine sediments from the Ross Sea and Weddell Seas by various researchers [Weiterman and Russell, 1986; Perry, 1999; Gerard-Little et al., 2006; Yeh et al., 2012]. In the Ross Sea, the sites where spherules have been reported extend southward from Cape Adare into Mc Murdo Sound (~750 km) and up to about 430 km off the coast of Victoria Land (Fig. 1; Table 3). Silica spherules have been identified in the DF 87-14 piston core [Perry, 1999] sampled in the western Ross Sea (Fig. 1) at depths of 142-140 and 122-120 cm b.s.f., and again at 62-60 and 40-38 cm b.s.f. (Fig. 3; Table 3). Radiocarbon dating on planktonic foraminifera from 5-9 cm and 140-141 cm b.s.f. yielded uncorrected ages >35.41 ka [Taviani et al., 1993] and <40.5 ± 1.5 ka BP [Smith and Licht, 2002], respectively (Table 3). To account for the uncorrected ages, a typical reservoir correction of 1300 ± 300 years, as recommended by Berkman and Forman [1996] for Southern Ocean biogenic carbonate samples, was applied. The corrected ages are >34.1 ± 0.3 and 39.2 ± 1.5 ka respectively. In Eltanin piston cores ELT32-8 and ELT32-43 recovered on the continental slope of the western Ross Sea, and in piston cores ELT32-13 and ELT32-16 collected off the Scott coast (Fig. 1; Table 3), spherules were identified in several sediment intervals [Perry, 1999; Gerard-Little et al., 2006], as illustrated in Figure 3. Age constraints are only provided for core ELT32-43, in which spherules occur in the sediment intervals 282-200 cm, 140-100 cm and 41-43 cm b.s.f. [Perry, 1999]. For this core radiocarbon dating at 100-102 cm and 160-162 cm yielded corrected ages of 34.57 ± 0.79 and 23.8 ± 0.24 ka [Smith and Licht, 2002], respectively (Fig. 3; Table 3). Corrected radiocarbon ages of between ~11.15 and 7.30 ka BP (Fig. 3 and Table 3) were reported for spherule-bearing sediments at depths of 210-190 cm b.s.f. in the core NBP 95-01 39KC sampled in the mid-continental shelf of the western Ross Sea [Cunningham et al., 1999; Fig. 2]. Spherules have also been reported in calcareous ooze and fine sand throughout piston core DF 80-92, in the fine sands of piston core DF 80-117 (Fig. 3), and in the coarse sand and diatomaceous mud of grab samples DF 80-39, –49 and –77 [Weiterman and Russell, 1986; Fig. 3]. A Quaternary age is reported for grab sample DF 80-39, as well as for piston cores DF 80-92 and –117 at depths of 95-96 and 35-36 cm b.s.f., respectively [Amrisar et al., 1988]. No spherules were found in Ross Sea marine sediments younger than ~7.3 ka BP.

Core	Lat. (S) Long. (E)	Depth [cm b.s.f.]	Age	Reference
ANTA02-NW02	Lat.: −73.516° Long.: 170.550°	133	23.7 ± 5.3 - 72 ± 2.8 ka cal. BP	Del Carlo et al. [2015]
ANTA02-NW03	Lat.: −72.967° Long.: 170.989°	104-103	33.5 - 33.96 ka cal. BP	This work
		54-55	24.76 - 25.37 ka cal. BP	Del Carlo et al. [2015]
		12-0	15.45 - 15.84 ka cal. BP	This work
ANTA99-NW27	Lat.: −72.994° Long.: 172.091°	168.5-18.5	<30.3 ka cal. BP	Colizza et al. [2003]
ANTA99-NW31	Lat.: −73.227° Long.: 170.988°	89-14.5	<24.1 ka cal. BP	Colizza et al. [2003]
DF87-14	Lat.: −72.972° Long.: 179.892°	38-40	>35.41 ka BP and <40.5 ± 1.5 ka (uncorrected)	Taviani et al. [1993]; Smith and Licht [2002]
		60-62		
		122-120		
		142-140		
EL32-08	Lat.: −73.967° Long.: 176.117°	10	—	
EL32-13	Lat.: −74.955° Long.: 172.163°	22-20	—	
		100-98	—	
		122-120	—	
		184-182	—	
EL32-16	Lat.: −75.973° Long.: 178.137°	62-60	—	
		82-80	—	
		100-98	—	
		122-120	—	
		142-140	—	
		162-160	—	
		182-180	—	
		282-280	—	
EL32-43	Lat.: −72.453° Long.: 176.983°	43-41	—	
		102-100	<34.57 ± 0.79 ka and >23.85 ± 0.24 ka cal. BP	Smith and Licht [2002]
		122-120		
		142-140		
		202-200	—	
		242-240	—	
		262-260	—	
		282-280	—	
NBP95-01 30KC	Lat.: −76.058° Long 164.585°	—	—	
NBP95-01 31KC	Lat.: −75.7° Long 165.417°	—	—	
NBP95-01 37KC	Lat.: −74.498° Long 167.743°	—	—	

Core	Lat. (S) Long. (E)	Depth [cm b.s.f.]	Age	Reference
NBP95-01 39KC	Lat.: −74.024° Long 172.961°	210-190	<11.15 and >7.30 ka cal. BP	Cunningham et al. [1999]
NBP 99-02 11KC	Lat.: −76.311° Long 169.659°	—	—	
NBP 99-02 12KC	Lat.: −76.312° Long 169.668°	—	—	
DF80 - 39 (grab)	Lat.: −71.017° Long.: 168.733°	—	—	
DF80 - 49 (grab)	Lat.: −77.31° Long: 164.44°	—	—	
DF80 - 92	Lat.: −75.33° Long: 163.02°	0-117	—	
DF80 - 117	Lat.: −74.53° Long.: 164.04°	0-30	—	
IWSOE68 68-16	Lat.: −74.85° Long.: −39.083°	—	—	
IWSOE70 2-19-2	Lat.: −74.35° Long.: −38.25°	30-35	16.19 ± 0.07 ka cal. BP	Smith and Licht [2002]
		350-355	15.09 ± 0.27	Hillenbrand et al. [2012]

Table 3. Sampling details of cores where silica spherules have been found with sediment depths and ages of sediment layers indicated.

Silica spherules were found also in sediments of the Weddell Sea; specifically, cores IWSOE70 2-19-1 and IWOE68-16 (Fig. 1) document their occurrence but without a precise indication of sediment depths [Perry, 1999]. In core IWSOE70 2-19-1, consisting mostly of unstratified to stratified pebbly mud, radiocarbon ages on foraminifera yielded downcore inverse uncorrected ^{14}C ages of 16.19 ± 0.07 and 11.27 ± 0.06 ka at a depths of 30-35 cm and 350-355 cm b.s.f., respectively [Anderson and Andrews, 1999; Smith and Licht, 2002]. Smith and Licht [2002] emphasise that the younger age should not be considered due to it being obtained from mixed benthic and planktonic foraminifera, whereas the older age was derived solely from benthic foraminifera, making it more reliable. The latter age has been later calibrated to yield a corrected age of 15.09 ± 0.27 ka BP [Hillenbrand et al., 2012]. No age is provided for Weddell Sea core IWOE68-16.

5. Discussion

5.1 Concentrically layered silica spherules vs unstructured silica-rich spherules: similarities and differences

Silica-rich spherules are widespread in many geologic records on Earth [Generau et al., 2015] and have also been identified on the Moon [McGetchin and Head, 1973; Heiken et al., 1974; Heiken and McKay, 1978; Heiken and Wohletz, 1985]. These are formed through a range of natural processes, primarily at high temperatures.

When a meteorite from space enters the atmosphere and melts upon impact, it generates cosmic spherules [e.g., Brownlee et al., 1983; Genge et al., 2008; Generau et al. 2015]. Similarly, the high-energy impact of an extra-terrestrial object on Earth's surface may instantaneously melt and vaporise the impacted substratum, leading to the formation of spheroidal, glassy, sand-sized particles known as microtektites [Simonson and Glass, 2004; Glass and Simonson, 2013].

Glassy spherules (achneliths) are produced by volcanic processes, resulting from the spray of hot, low-viscosity magmas during basaltic eruptions [Walker and Croasdale, 1971; Carracedo Sánchez et al., 2010; Porritt et al., 2012] or from the alteration of volcanic glass in eruptive columns [Lefèvre et al., 1986; Spadaro et al., 2002].

Silica spherules are created when the heat generated by a cloud-to-ground lightning strike melts the substrate [Pasek et al., 2012; Generau et al., 2015].

However, the geochemical composition and concentric layering of the silica spherules studied in this work have distinct characteristics that differentiate them from other silica-rich spherules produced by high-temperature natural processes, hitherto known. In the following section, we summarise the physical features and chemical

composition of the latter and discuss how they differ from those studied here. Specifically, we focus on silica-rich, glassy spheroidal particles, excluding metallic or other non-glassy spherules (e.g. clinopyroxenes spherules).

Cosmic spherules and microtektites

Cosmic spherules and microtektites can have variable internal textures [Genge et al., 2008; Glass and Simonson, 2013]. Microtektites are predominantly spherical [62 to 90% of the total; Glass and Simonson 2013 and references therein], but they can also take the form of teardrops, dumbbells, oblate shapes, or complex disks formed by the fusion of two or more microtektites. The size of microtektites ranges from a few tens of microns up to several millimetres, typically less than a millimetre in diameter. They come in a range of colours from transparent colourless to pale yellow, yellow, bottle green, or dark brown, with varying levels of opacity or translucency. The external surface of microtektites displays diverse textures such as protrusions, etching marks, corrosion, or high-velocity impact pits [Glass and Simonson, 2013 and references therein]. Internally, they are structureless, occasionally showing small vesicles, tiny crystalline phases, and silica-rich or lechatelierite inclusions [Glass and Simonson, 2013 and references therein]. The composition of microtektites varies widely; Cenozoic microtektites are typically SiO_2-rich with silica content varying from less than 50 wt% to over 80 wt%, with other major oxides decreasing proportionally with increasing silica. A notable characteristic of microtektites is their extremely low water content commonly <0.02 wt% [Glass and Simonson, 2013].

Achneliths

Achneliths produced by volcanic eruptions typically have a shiny appearance ranging in colour from honey-coloured to black and vary in shape from spherical to elongated. The external surface is usually smooth but may exhibit micro-cracks (polygonal), sinuous fine corrugations and wrinkles, or adhering dust. In thin sections, volcanic glass forming these particles can range from dense (unstructured) to highly vesicular and aphyric to microlite-rich. Volcanic glass may undergo alteration into palagonite, resulting in an orange colour. The chemical composition of achneliths is mostly basaltic with SiO_2 between 45-52 wt%, total alkali content ($K_2O + Na_2O$) <5 wt%. The average chemical composition of basalt determined by 3594 chemical analyses of basaltic rocks recalculated volatile-free to a total of 100% is available in Best [2002].

Fulgurite droplets

Fulgurite droplets are particles expelled from a fulgurite formed by cloud-to-ground lightning strikes [Pasek et al., 2012]. They have a fused and fluidal external morphology, while internally they are typically solid, often containing unmelted mineral grains, vesicles, or voids. The composition of fulgurite droplets generally mirrors the composition of the substrate targeted by the lighting. Usually, they consist of coexisting nearly pure SiO_2 glass (lechatelierite) coexisting with a second melt composed of a mixture of the other oxides [groundmass melt; Pasek et al., 2012]. Microprobe analyses of fulgurite, similar to cosmic spherules and microtektites, indicate a relatively low water content of less than <1 wt%.

From the discussion above, it is evident that the silica spherules examined in this study differ from any spherical particles produced by natural processes at high temperatures both in terms of internal texture and chemical composition. Specifically, no fine or distinct layering has been identified in microtektites, cosmic spherules, achneliths, or fulgurite droplets. Similarly, the chemical composition of spherical particles created by natural processes at high temperatures differs from the silica spherules studied here. While there are microtektites with silica content comparable to the spherules analysed in our study (up to ~80 wt%), these are nearly water-free, with the remaining 20 wt% composed of other major oxides.

Furthermore, the external surface of the examined spherules is nearly perfectly smooth or may display small cracks and indentations, unlike other particles generated by natural phenomena at high temperatures, where external surfaces often exhibit protrusions, corrosion, and various types of impact pits. In this context, the silica spherules studied in this work and those found in the Ross and Weddell Seas sharing similar characteristics, cannot be associated with microtektites as suggested by Gerard-Little et al. [2006].

5.2 Hypothesis for the mechanism of formation of silica spherules

As mentioned above, the results indicate that spherules are not specific to particular sediment facies and are found in sediment sequences primarily representing sedimentation during interglacial periods characterised by open-sea conditions or limited sea ice coverage.

Based on the age constraints established for the analysed cores and those documented in existing literature, it is evident that spherules did not form continuously over time but rather during distinct intervals. Spherules occur at: 1) between 39.2 and approximately 34.57 ka; 2) between ~34.57 and 33.05-33.96 ka; 3) between ~25.4 and 21.2 ka; 4) slightly younger than 15.45-15.84 ka and 5) between 11.15 and 7.3 ka BP. The most recent sediments containing spherules are around 7.3 ka old.

The texture (both internal and external) and composition of the silica spherules analysed in this study suggest an origin not related to high-temperature natural processes. Conversely, several low-temperature natural processes could lead to the formation of spherules, including chemical, physical or biological mechanisms. Additionally, due to their layered structure, the occurrence of these spherules may be linked to cyclical processes of silica precipitation, as also proposed for layered granules in modern marine and terrestrial environments. A similar hypothesis was put forward in an early, purely descriptive study by Weiterman and Russell [1986], suggesting that silica spherules found in Ross Sea sediments could form through a cyclical chemical process. However, these authors did not specify the conditions under which these particles could form or the dynamics of their formation. In subsequent work, Perry [1999] speculated that spherules form through the inorganic precipitation of silica when silica-rich freshwater, resulting from ice melting, mixes with ocean waters. Perry dismissed the idea that spherules formed during regional-scale melting events associated with ice shelf retreat, as she found spherules only in areas of the Ross Sea and Weddell Sea where sea ice is seasonal. She proposed that the spherules formed when melting seasonal sea ice causes fresh water to mix with ocean water.

Several authors have suggested that the inorganic precipitation of silica on a large scale is responsible for the formation of cherts and iron-banded deposits during Archean times [Maliva et al., 2005; Posth et al., 2008]. Stefurak et al. [2015] propose that sand-sized silica granules forming Archean cherts may have formed through multistage aggregation of silica in systems with near-neutral to moderately alkaline pH and high concentrations of dissolved silica, triggered by rapid variation of silica concentration and salinity. Similarly, in modern environments, inorganic precipitation of silica occurs with significant fluctuation in pH. For instance, Jones et al. [1967] argued that silica-rich, high-pH (>10) brine forms when water reacts with silicates in closed basins and volcanic terrains, leading to the inorganic precipitation of large amounts of silica upon dilution with less alkaline waters. It is worth mentioning that, normally, secondary phases like silica nucleate on existing grains and grow as cement because the kinetic barrier is lower [Benning and Waychunas, 2007 and references therein]. In this case, spherules are forming without an obvious nucleation point. In this context, it cannot be ruled out that silica precipitation may have been facilitated by microbial activity capable of overcoming kinetic barriers and promoting mineral precipitation [Furukawa and O'Reilly, 2007], especially in conditions of high silica concentration and elevated pH values [Orange et al., 2009].

On these bases, we propose the hypothesis that spherules could form when variations in the physical and chemical properties (such as pH, temperature, salinity, etc.) of seawater are induced (Fig. 4). If spherules were to form through the inorganic precipitation of silica when silica-rich freshwater, resulting from seasonal ice melting, mixes with ocean waters as suggested by Perry [1999], we would expect to find spherules consistently throughout sediment sequences up to modern times. However, as indicated by our research, this did not occur, and spherules are constrained within specific time intervals, with the most recent dating back to around 7.3 thousand years Before Present (BP).

In the Ross Sea, the primary processes that could have triggered variations in the physical and chemical properties of seawater, thereby influencing the construction of spherules, include: 1) changes in bottom circulation, such as alterations in the efficiency of High Salinity Shelf Waters (HSSW) formation and the intrusion of Circumpolar Deep Waters (CDW) onto the continental shelf, or 2) changes in ice coverage and the melting of ice masses with the consequent contribution of amorphous silica-rich sediment trapped in the basal ice.

Two distinct time intervals characterised by increased nutrient supply and indicative of enhanced upper CDW upwelling were identified near Cape Adare, approximately around 15-10 ka and 7.5-6 ka [Langone et al., 2010]. However, these periods do not appear to be directly associated with any spherule formation events, with the last known occurrence falling between 11.15 and 7.30 ka BP, just between these two intervals.

The most recent period of spherule formation aligns closely with the last retreat of the grounding line in the western Ross Sea, which occurred between approximately 11 and 6 ka [Domack et al., 1999], significantly contributing to meltwater pulse 1B [Fairbanks, 1989; Liu and Milliman, 2004; Peltier and Fairbanks, 2006; Deschamps et al., 2012]. Furthermore, the second youngest period of spherule formation, dated younger than 15.45-15.84 ka BP, is not too far from the age of meltwater pulse 1A around ~14.3-14.0 ka BP [Liu and Milliman, 2004], which was notably intense in this region of Antarctica [Clarke et al., 1996].

Moreover, the absence of silica spherules in sediments younger than 7.30 ka BP, corresponding to the time when the Ross Ice Shelf reached its present-day position near Ross Island, strengthens the hypothesis that large-scale ice melting events may be responsible for silica spherule precipitation. Variations in parameters such as salinity, pH, and silica saturation during the mixing of seawater with extensive meltwater masses, potentially influenced by the presence of bacteria [Davaud and Girardclos, 2001], together with the release of substantial amounts of silicate-rich sediment, may have created ideal conditions for spherule formation. A significant amount of silica could have been supplied through the chemical alteration of silicate minerals from bedrocks and aeolian dust trapped in the ice and later released into seawater during periods of heightened meltwater production [Stumpf et al., 2012 and references therein].

The spherical shape and thin, concentric layering of spherules may result from the cyclical precipitation of silica during particle movement within a relatively turbulent hydrodynamic regime. Such regimes could occur in vortices or turbulent eddies during turbulent mixing of seawater with freshwater, as well as in strong bottom currents greater than 1 m/s [Budillon et al., 2011], like those observed in the Drygalski Trough (Fig. 4).

Before the last deglaciation, correlating spherule occurrence with meltwater pulses is more challenging due to age biases present in both sediment records and meltwater pulse chronology. Nevertheless, a rough correlation exists between periods of spherule formation and sea-level rises induced by meltwater pulses, as reconstructed from dating Pacific reef terraces by various researchers [Chappell et al., 1996; Blanchon, 2011].

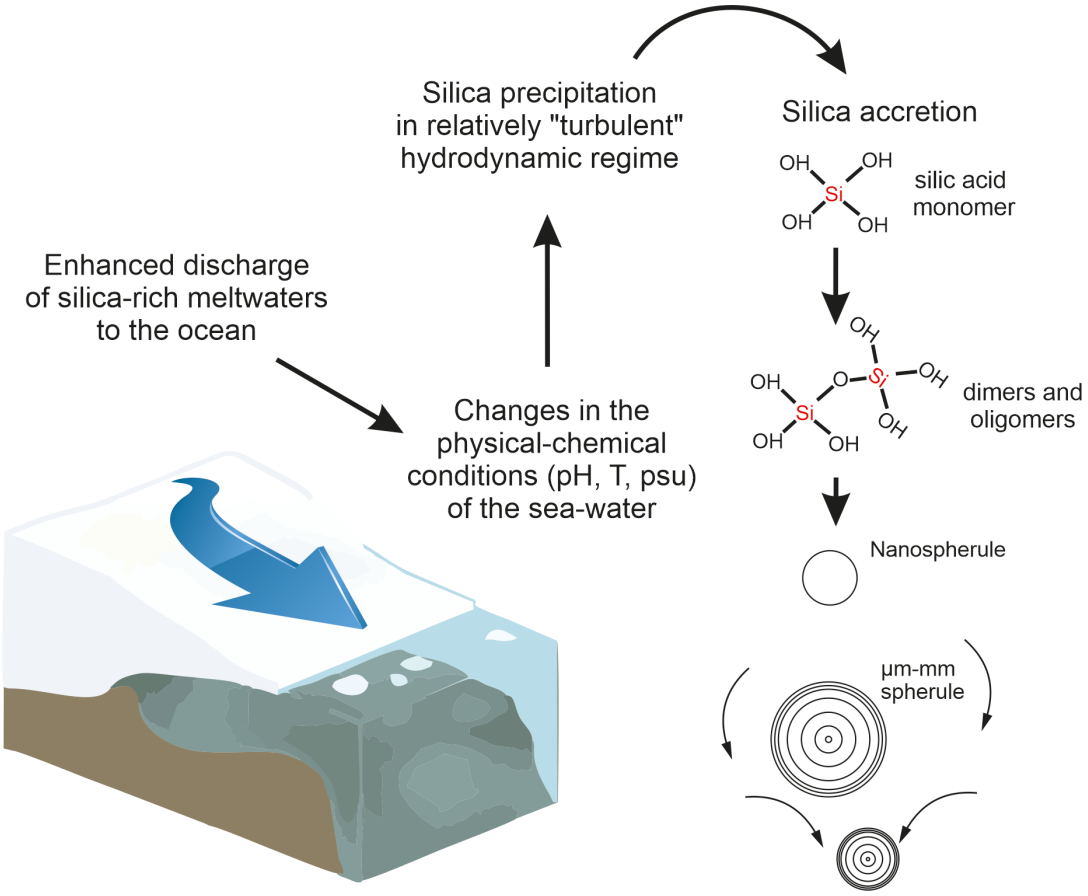

Figure 4. Schematic representation of how the spherules may form due to strong changes in parameters such as salinity, pH and silica saturation during the mixing of seawater with meltwater.

6. Conclusive remarks

We have described distinct silica spherules found in glaciomarine sediments from the Ross Sea, which closely resemble those previously identified in various cores from the Ross and Weddell Seas. These spherules are present in sediments deposited during open-sea conditions or with limited sea ice coverage. The conditions that led to spherule formation recurred approximately every 5-10 thousand years, in a period between around 39.2 to 7.3 thousand years ago. The two most recent sediment intervals containing spherules are dated to <15.84 thousand years ago and 11.15-7.30 thousand years ago, aligning with the timing of meltwater pulses 1A and 1B in the West Antarctic Ice Sheet.

Through sedimentological, textural, and chemical analysis of the spherules, along with a review of literature data and radiocarbon dating of sediments, we have developed a general hypothesis regarding the possible mechanism of formation of these silica spherules. We suggest that the spherules originated from the precipitation of inorganic silica during significant discharges of silica-rich freshwater into the ocean, likely triggered by extensive ice melting events possibly that occurred during climatic fluctuations in Antarctica. This process is not believed to be associated with seasonal sea ice melting, as previously suggested by Perry [1999].

Further investigations of Antarctic marine sediment records focusing on identifying and dating spherules could enhance their regional correlation, potentially serving as a proxy for substantial production and discharge of meltwater into the ocean. Combining this proxy with other independent global and local climatic indicators could enhance our understanding of past ice sheet dynamics.

Acknowledgements. This work was funded by the Italian Programma Nazionale di Ricerche in Antartide, PdR2010/A2.12.

References

Amrisar, F.K., M.D. Russell, S.D. Weiterman, C.R. Cooper, D.R. Clarck, J.M. Covington, J.L. Firth, Applegate, S. Knüttel and J.R. Breza (1988). In Cassidy, D.S. (ed.), The United States Antarctic research program in the Western Ross Sea, 1979-1980: The sediment descriptions, Antarctic Marine Geology Research facility, Florida State University, Sedimentology Research Laboratory Contribution 53, 1-230.

Anderson, J.B and J.T. Andrews (1999). Radiocarbon constraints on ice sheet advance and retreat in the Weddell Sea, Antarctica, Geology, 27, 2, 179-182. https://doi.org/10.1130/0091-7613(1999)027<0179:RCOISA>2.3.CO;2

Anderson, J.B., H. Conway, P.J. Bart, A.E. Witus, S.L. Greenwood, R.M. McKay, B.L. Hall, R.P. Ackert, K. Licht, M. Jakobsson and J.O. Stone (2014). Ross Sea Paleo-Ice Sheet Drainage and Deglacial History During and Since the LGM, Quat. Sci. Rev., 100, 31-54, https://doi.org/10.1016/j.quascirev.2013.08.020

Benning, L. and G. Waychunas (2008). Nucleation, Growth, and Aggregation of Mineral Phases: Mechanisms and Kinetic Controls. In: Brantley, S., Kubicki, J., White, A. (eds) Kinetics of Water-Rock Interaction. Springer, New York, NY. https://doi.org/10.1007/978-0-387-73563-4_7

Berkman, P.A. and S.L. Forman (1996). Pre-bomb radiocarbon and the reservoir correction for calcareous marine species in the Southern Ocean, Geophys. Res. Let., 23, 363-366. https://doi.org/10.1029/96GL00151

Best, M.G. (2002). Igneous and Metamorphic Petrology, 2nd Edition. Wiley-Blackwell.

Blanchon, P. (2011). Meltwater Pulses, In: Hopley, D. (ed.), Encyclopedia of Modern Coral Reefs: Structure, form and process, Springer-Verlag Earth Science Series, 683-690. https://doi.org/10.1007/978-90-481-2639-2_232

Brownlee, D.E., B. Bates and R.H. Beauchamp (1983). Meteor ablation spherules as chondrule analogs, In: King, E.A., ed., Chondrules and their origins: Houston, Texas, Lunar and Planetary Institute, 1, 10-25.

Budillon, G., P. Castagno, S. Aliani, G. Spezie, L. Padman (2011). Thermohaline variability and Antarctic bottom water formation at the Ross Sea shelf break, Deep-Sea Res. I: Oceanogr. Res. Pap., 58, 1002-1018. https://doi.org/10.1016/j.dsr.2011.07.002

Carracedo Sánchez, M., J. Arostegui, F. Sarrionandia, E. Larrondo and J.I. Gil Ibarguchi (2010). Cryptoachneliths: Hidden glassy ash in composite spheroidal lapilli, J. Volcanol. Geoth. Res., 196, 77-90. https://doi.org/10.1016/j.jvolgeores.2010.07.009

Chappell, J., A. Omura, T. Esat, M. McCulloch, J. Pandolfi, Y. Ota and B. Pillans (1996). Reconciliation of late Quaternary sea levels derived from coral terraces at Huon Peninsula with deep sea oxygen isotope records, Earth Plan. Sci. Let., 141, 227-236. https://doi.org/10.1016/0012-821X(96)00062-3

Clarke, P.U., R.B. Alley, L.D. Keigwin, J.M. Licciardi, S.J. Johnsen and H. Wang (1996). Origin of the first global meltwater pulse following the last glacial maximum, Paleoceanography, 11, 563-577. https://doi.org/10.1029/96PA01419

Colizza, E., F. Finocchiaro, L. Marinoni, L. Menegazzo Vitturi and A. Brambati (2003). Tephra evidence in marine sediments from the shelf of the Western Ross Sea, Terra Ant., 8, 121-126.

Cunningham, W.L., A. Leventer, J.T. Andrews, A.E. Jennings and K.J. Licht (1999). Late Pleistocene-Holocene marine conditions in the Ross Sea, Antarctica: evidence from the diatom record, The Holocene, 9, 129-139. https://doi.org/10.1191/095968399967562479

Davaud, E. and S. Girardclos (2001). Recent Freshwater Ooids and Oncoids from Western Lake Geneva (Switzerland): Indications of a Common Organically Mediated Origin, J. Sed. Res., 71, 423-429. https://doi.org/10.1306/2DC40950-0E47-11D7-8643000102C1865D

DeMaster, D.J., (1981). The supply and accumulation of silica in the marine environment, Geochim. Cosmochim. Acta, 45, 1715-1732. doi:10.1016/0016-7037(81)90006-5. https://doi.org/10.1016/0016-7037(81)90006-5

Deschamps, P., N. Durand, E. Bard, B. Hamelin, G. Camoin, A.L. Thomas, G.M. Henderson, J. Okuno and Y. Yokoyama (2012). Ice-sheet collapse and sea-level rise at the Bølling warming 14,600 years ago, Nature, 483, 559-564. https://doi.org/10.1038/nature10902

Del Carlo, P., A. Di Roberto, G. Di Vincenzo, A. Bertagnini, P. Landi, M. Pompilio, E. Colizza and G. Giordano (2015). Late Pleistocene-Holocene volcanic activity in northern Victoria Land recorded in Ross Sea marine sediments (Antarctica), Bull. Volcanol., 77, 36. https://doi.org/10.1007/s00445-015-0924-0

Domack, E.W., E.A. Jacobson, S. Shipp and J.B. Anderson (1999). Late Pleistocene-Holocene retreat of the West Antarctic Ice – Sheet system in the Ross Sea: Part 2 – Sedimentologic and stratigraphic signature. Geol. Soc. Am. Bull., 111, 1517-1536. https://doi.org/10.1130/0016-7606(1999)111<1517:LPHROT>2.3.CO;2

Furukawa, Y. and S.E. O'Reilly (2007). Rapid precipitation of amorphous silica in experimental systems with nontronite (NAu-1) and Shewanella oneidensis MR-1, Geochim. Cosmochim. Acta, 71, 363-377. https://doi.org/10.1016/j.gca.2006.09.006

Genereau, K., J.B. Wardman, T.M. Wilson, S.R. McNutt and P. Izabekov (2015). Lightning-induced volcanic spherules, Geology, 43, 319-322. https://doi.org/10.1130/G36255.1

Genge, M.J., C. Engrand, M. Gounelle and S. Taylor (2008). The classification of micrometeorites, Meteorit. Planet. Sci., 497-515. https://doi.org/10.1111/j.1945-5100.2008.tb00668.x

Gerard-Little, P., D. Abbott, D. Breger and L. Burckle (2006). Evidence for a Possible Late Pliocene Impact in the Ross Sea, Antarctica (abstract). Lunar and Planetary Science XXXVII, abstract 1399.

Glass, B.P. and B.M. Simonson (2013). Distal Impact Ejecta Layers: New York, Springer Heidelberg, 716. https://doi.org/10.1007/978-3-540-88262-6

Heiken, G. and D.S. McKay (1978). Petrology of a sequence of pyroclastic rocks from the Valley of Taurus-Littrow (Apollo 17 landing site), In: Proceedings, 9th Lunar and Planetary Science Conference, Houston, Texas, 13-17 March: Houston, Lunar and Planetary Institute, 1933-1943.

Heiken, G.H. and K. Wohletz (1985). Volcanic Ash. University of California Press, Berkeley, 245.

Heiken, G.H., D.S. McKay and R.W. Brown (1974). Lunar deposits of possible pyroclastic origin, Geochim. Cosmochim. Acta, 38, 1703-1718, https://doi.org/10.1016/0016-7037(74)90187-2

Hillenbrand, C-D., A. Melles, G. Kuhn and R.D. Larter (2012). Marine geological constraints for the grounding line position of the Antarctic Ice Sheets on the southern Weddell Sea shelf at the Last Glacial Maximum, Quat. Sci. Rev., 32, 25-47. https://doi.org/10.1016/j.quascirev.2011.11.017

Jones, B.F., S.L. Rettig amd H.P. Eugster (1967). Silica in Alkaline Brines, Science, 158, 1310-1314. http://doi.org/10.1126/science.158.3806.1310

Langone, L., A. Asioli, F. Tateo, F. Giglio, D. Ridente, V. Summa, A. Carraro, M.L. Giannossi, A. Piva and F. Trincardi (2010). Bottom water production variability in the Ross Sea slope during the Late Pleistocene-Holocene as revealed by benthic foraminifera and sediment geochemistry, Geophys. Res. Abs., 12, EGU2010-7848.

Lefèvre, R.A., A. Gaudichet and M.A. Billon Galland (1986). Silicate microspherules intercepted in the plume of Etna volcano, Nature, 322, 817-820. https://doi.org/10.1038/322817a0

Liu, J.P. and J.D. Milliman (2004). Reconsidering Melt-water Pulses 1A and 1B: Global Impacts of Rapid Sea-level Rise, J. Ocean U. China, 3, 2, 183-190. https://doi.org/10.1007/s11802-004-0033-8

Livingstone, S.J., C.Ó. Cofaigh, C.R. Stokes, C.-D. Hillenbrand, A. Vieli and S.S.R. Jamieson (2012). Antarctic palaeo-ice streams, Earth-Sci. Rev., 111, 90-128. https://doi.org/10.1016/j.earscirev.2011.10.003

Maliva, R.G., A.H. Knoll and B.M. Simonson (2005). Secular change in the Precambrian silica cycle: Insights from chert petrology, Geol. Soc. Am. Bull., 117, 835-845, https://doi.org/10.1130/B25555.1

McGetchin, T.R., M. Settle and J.W. Head (1973). Radial thickness variation in impact crater ejecta: Implications for lunar basin deposits, Earth Plan. Sci. Let., 20, 226-236. https://doi.org/10.1016/0012-821X(73)90162-3

Orange, F., F. Westall, J.R. Disnar, D. Prieur, N. Bienvenu, M. Le Romancer and C. Défarge (2009). Experimental silicification of the extremophilic Archaea Pyrococcus abyssi and Methanocaldococcus jannaschii: applications in the search for evidence of life in early Earth and extraterrestrial rocks, Geobiology, 7, 403-418. https://doi.org/10.1111/j.1472-4669.2009.00212.x

Pasek, M.A., K. Block and V. Pasek (2012). Fulgurite morphology: A classification scheme and clues to formation, Contrib. Mineral, Petrol., 164, 477-492. https://doi.org/10.1007/s00410-012-0753-5

Peltier, W.R. and R.G. Fairbanks (2006). Global glacial ice volume and Last Glacial Maximum duration from an extended Barbados sea level record, Quat. Sci. Rev., 25, 3322-3337. https://doi.org/10.1016/j.quascirev.2006.04.010

Perry, P.J. (1999). Quaternary benthic foraminiferal distribution in the Ross Sea, Antarctica, and its relationship to oceanography, Ph. D. Thesis, Louisiana State University, Baton Rouge, 358 p.

Porritt, L.A., J.K. Russell and S.L. Quane (2012). Pele's tears and spheres: Examples from Kilauea Iki, Earth Plan. Sci. Let., 333-334, 171-180. https://doi.org/10.1016/j.epsl.2012.03.031

Posth, N.R., F. Hegler, K.O. Konhauser and A. Kappler (2008). Alternating Si and Fe deposition caused by temperature fluctuations in Precambrian oceans, Nature Geosci., 1, 703-708. https://doi.org/10.1038/ngeo306

Shipp, S., J.B. Anderson, E.W. Domack (1999). Seismic signature of the Late Pleistocene fluctuation of the west Antarctic ice sheet system in Ross Sea: a new perspective, Part I. Bulletin of the Geol. Soc. Am., 111, 1486-1516. https://doi.org/10.1130/0016-7606(1999)111<1517:LPHROT>2.3.CO;2

Simonson, B.M. and B.P. Glass (2004). Spherule layers-records of ancient impacts, Annu. Rev. Earth Planet. Sci., 32, 329-361. https://doi.org/10.1146/annurev.earth.32.101802.120458

Smith, M. and K. Licht (2002). Radiocarbon date list IX: Antarctica, Arctic Ocean, and the Northern North Atlantic. Occasional paper 54, Institute of Arctic and Alpine Research, University of Colorado, Boulder, Colorado.

Spadaro, F.R., R.A. Lefèvre R.A. and P. Auset (2002). Experimental rapid alteration of basaltic glass: implications for the origins of atmospheric particulates, Geology, 30, 671-674. https://doi.org/10.1130/0091-7613(2002)030<0671:ERAOBG>2.0.CO;2

Stefurak, E.J.T., R.D. Lowe, D. Zentner and W.W. Fischer (2015). Sedimentology and geochemistry of Archean silica granules, Geol. Soc. Am. Bull., 127, 7-8, 1090-1107. https://doi.org/10.1130/B31181.1

Stumpf, A.R., M.E. Elwood Madden, G.S. Sorghan, B.L. Hall, L.J. Keiser, K.R. Marra (2012). Glacier meltwater stream chemistry in Wright and Taylor Valleys, Antarctica. Significant roles of drift, dust and biological processes in chemical weathering in a polar climate, Chem. Geol., 322-323, 79-90. https://doi.org/10.1016/j.chemgeo.2012.06.009

Taviani, M., D.M. Reid and J.B. Andreson (1993). Skeletal and isotopic composition and paleoclimatic significance of Late Pleistocene carbonates, Ross, Sea, Antarctica, J. Sediment. Petrol., 63, 84-90. https://doi.org/10.1306/D4267A96-2B26-11D7-8648000102C1865D

Walker, G.P.L. and R. Croasdale (1971). Characteristics of some basaltic pyroclasts, Bull. Volcanol., 35, 303-317. https://doi.org/10.1007/BF02596957

Weiterman, S.D. and J.R. Russell (1986). Siliceous ooids from Antarctic marine sediments, Antarct. J. U.S., 21, 159-160.

Yeh, C., D.H. Abbott, M.H. Anders and D. Breger (2012). What is the Age and Origin of the Spherule Bearing Layer in some Ross Sea Cores? AGU Fall Meeting 1, 1787.

***CORRESPONDING AUTHOR: Alessio DI ROBERTO**

Istituto Nazionale di Geofisica e Vulcanologia, Sezione di Pisa, Via C. Battisti 53, 56125 Pisa, Italy,

e-mail alessio.diroberto@ingv.it